

§4. Extraction of Spatial Plasma Structures by Analyzing Fluctuations in Core and Edge of GAMMA 10

Tanaka, H.,
Sakamoto, M., Mizuguchi, M., Oki, K., Yoshikawa, M.,
Nojiri, K., Nohara, R., Terakado, A., Kohagura, J.,
Yoshikawa, M. (Univ. Tsukuba),
Ohno, N., Tsuji, Y. (Nagoya Univ.)

The tandem mirror device GAMMA10 has common magnetic field lines in the central (core) and end (edge) regions. This study aims to clarify the interdependency between the core and edge plasmas for improving controllability and performance from the statistical analyses of electrostatic fluctuations. In order to measure the core-plasma fluctuation, we used the gold neutral beam probe (GNBP)¹⁾. Further, edge fluctuations were acquired by the target plate, the end plate, and/or Langmuir probes inside the divertor module.

In the past collaboration research, we had estimated propagation speeds along/across the magnetic field of a periodic fluctuation; however, we couldn't identify the instability and this phenomenon was not reproducible well²⁾. In fiscal year 2014, we have investigated the reproducibly-observed flute instability during an application of plug/barrier-electron cyclotron heating (P/B-ECH) period³⁾.

Figure 1 shows power spectra of the plasma potential (V_p) measured by the GNBP and the target-plate potential (V_t), which was shorted with a 150 Ω resistor, in the P/B-ECH period. Measurement position of the GNBP was vertically swept from $x \sim -3.5$ cm to ~ 15 cm at 50 Hz. On the other hand, the target plate was fixed at radially center. Sampling frequency of V_p and V_t was 1 MHz. Spectral peaks can be found at $f \sim 5.6$ kHz in both spectra, which are attributable to the flute instability.

In order to obtain the spatial behavior of the instability, radial distribution of the phase delay is one of the important elements. In this experiment, the flute instability was stably observed only at $t = [147, 168]$ ms (= \sim one period of the GNBP sweeping) and the ~ 5.6 kHz fluctuation appeared only in three periods while x varies ~ 1 cm. Therefore, we employed the wavelet transform that is effective technique for such a non-steady signal analysis.

Figure 2(a) shows x and the wavelet coefficients of V_p and V_t at $f \sim 5.6$ kHz. Time series and dependence on x of the phase difference between V_p and V_t are shown in Figs. 2(b) and (c), respectively. When an intensity of the wavelet coefficient is small, error of its phase calculation becomes large. Thus, the phase difference during the wavelet coefficient of V_t exceeding $(\mu - \sigma)$ are over-plotted with thick curves in Figs. 2(b) and (c), where μ and σ indicate the mean and the standard deviation, respectively. From the thick line in Fig. 2(c), the phase difference is found to trace a nearly common trajectory during a round-trip of x .

This study demonstrated an estimation of the radial distribution of the phase difference between potential signals measured by the movable GNBP and the fixed target plate from a discharge, which indicates the radial distribution of V_p . To improve validity of this result, a longer steady state signal is needed.

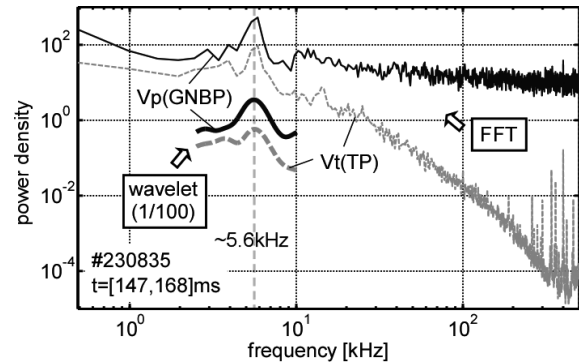


Fig. 1. Fourier power spectra (thin lines) of V_p (solid line) and V_t (dashed line). Wavelet spectra (thick lines) are also depicted.

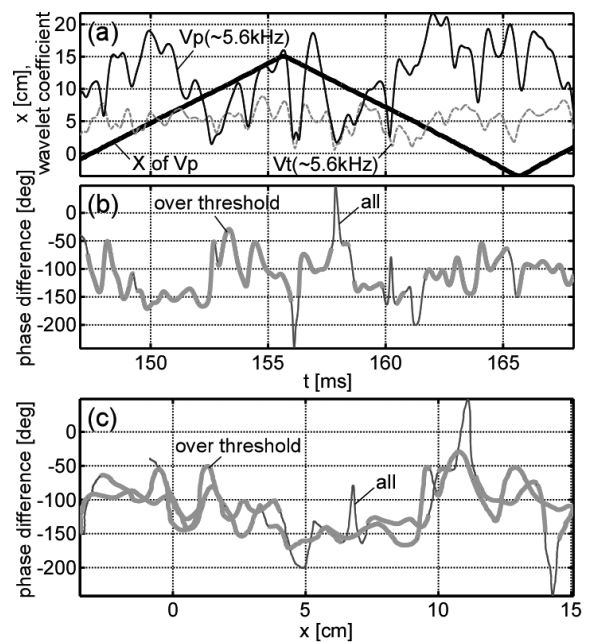


Fig. 2. (a) Time series of the vertical position x (thick solid line) and the wavelet coefficients of V_p (thin solid line) and V_t (thin dotted line) at $f \sim 5.6$ kHz. (b) Phase difference between the $f \sim 5.6$ kHz components of V_p and V_t (thin line). (c) The phase difference as a function of x . Lines during the wavelet coefficient of V_t exceeding $(\mu - \sigma)$ are over-plotted as thick lines in Figs. (b) and (c).

- 1) Mizuguchi, M. et al.: Rev. Sci. Instrum. **79** (2008) 10F309.
- 2) Tanaka H. et al.: *accepted in Fusion Sci. Technol.*
- 3) Yaguchi F. et al.: Fusion Sci. Technol. **59** (2011) 253.